Mansoura Engineering Journal

Volume 12 | Issue 1 Article 12

6-1-2021

Effect of Nature of the Surface of the Condensate Film on Condensation Heat Transfer.

Mohamed Mahgoub
Assistant Professor of Mechanical Power Engineering Department, Faculty of Engineering, Mansoura University, Mansoura, Egypt., magnerm@mans.edu.eg

Recommended Citation

Mahgoub, Mohamed (2021) "Effect of Nature of the Surface of the Condensate Film on Condensation Heat Transfer.," *Mansoura Engineering Journal*: Vol. 12 : Iss. 1 , Article 12.
Available at: https://doi.org/10.21608/bfemu.2021.174534

EFFECT OF NATURE OF THE SURFACE OF THE CONDENSATE FILM ON CONDENSATION HEAT TRANSFER

By

M. Mahgoub

EL-Mansoura University

خلاصة ـ فى هذا البحث التحليلى يتم دراسة تأثير طبيعة سطح طبقة التكثيف على معامل الانتقال الحرارى أثناء التكثيف الرقائقى للأبخرة ، وذلك لأنّ سطح طبقة التكثيف ليس مستو كما فرض فى نظرية نسلت ، ولكن هذا السطح ذو طبيعة موجية معقدة ، وفى هذا العمل تم فرض طبيعة موجية بسيطة ، ثم تمت دراسة تأثير خصائص هذه الطبيعة الموجية على قيمة معامل الانتقال الحرارى للتكثيف ، حيث وجد أنه كلما كان تردد الموجة السطحية كبيرا كلما زاد معامل الانتقال الحرارى المتوسط لسطح مستوى حيث تقرب قيمته لنظيرتها فى التكثيف على هيئة قطرات .

ABSTRACT- This paper is concerned with the investigation of the effect of the nature of the surface of the condenste film on heat transfer during laminar film condensation. An idealized rippled nature of the film surface is proposed. Local heat transfer coefficients are calculated for film condensation on a vertical plate in laminar case. Calculations are performed numerically. For the proposed rippled nature of the film surface, the average heat transfer coefficients are up to 20% higher than that obtained for smooth surface.

INTRODUCTION

Design of total or partial condensers for single vapor or multicomponent mixture is one of the important problems in the field of thermal and chemical engineering.

Laminar film condensation has been described and analyzed by Nusselt [1,2] under several simplifying assumptions such as :

1- acceleration effects in the liquid film are ignored;
2- linear temperature distribution in the film is assumed ;
3- energy effect of liquid subcooling is not included.

Nusselt analysis has been later improved by many investigators to account for the above mentioned effects. Also, boundary layer analysis has been applied to film condensation. Boundary layer analysis improves the accurcy of the representation of the film condensation process by including convection terms in the liquid layer.

In many circumstances, actual transfer rates are substantially higher than predicted ones [2]. These discrepancies have been explained to arise mainly because the behaviour of the actual film differs from that assumed. Many actual films flow in a rippled manner [4,5]. These ripples often arise because of such disturbances as uneven, though small, vapor velocities or as a result of condensate drainage from higher surfaces. The effect of this rippled structure is to increase the heat transfer rate. Considering Fig. 1, The sensible heat flux q_g from the bulk of gas phase is given by :

$$q_g = h_g \; (t_g - t_s) , \qquad \ldots (1)$$

where h_g is the dry gas heat transfer coefficient, which is generally evaluated as if the gas phase were flowing alone [3]. The local overall heat transfer coefficient U, defined by

$$q_t = U (t_g - t_w) = h_f (t_s - t_w) . \qquad \ldots (2)$$

is then given by

$$(1/U) = (1/h_f) + q_g/h_g q_t , \qquad \ldots (3)$$

where q_t is the total heat flux and h is the condensate film heat transfer coefficient.

To determine the dry gas heat transfer coefficient, there are many correlations which give acceptable values for laminar and tubulent flow of gas phase [1,2]. Such correlations apply to smooth surface. Wall roughness, which increases pressure loss by promoting momentum transfer, also increases heat transfer. Nunner, 1956 carried out extensive tests on air in tubes whose inside surfaces were artificially roughened [2]. It was found that the Nusselt number for the roughened wall is a function of the flow Reynolds number and of the ratio of the actual friction factor and the friction factor for smooth-wall flow at the same Reynolds number as shown in Fig. 2 and expressed by the following relation [4]:

$$Nu = 0.125 \, Re \, Pr \, /(1 + 1.5 \, Re^{-0.125} \, Pr^{-0.1667} \, (Prf/f_o - 1), \qquad \ldots (4)$$

where f_o is the friction factor obtained from Blassius equation for smooth surface

$$f_o = (100 \, Re)^{-0.25} \qquad \ldots (5)$$

Now, in the process of film condensation, the surface of the condensate film builds the tube wall, whose structure effects the heat transfer process. This effect may be compared with the effect of the surface roughness with two main differences :

1- The condensate has a velocity relative to the vapor phase; and
2- the ripple characteristics are not constant along the way of flow.

To determine the friction factor f (Eq.4) due to the roughness of the condensate film, Hempel developed the following correlation [4] :

$$f = f_o \, [1 + 17.2 \, (\delta_f / d_i)^{0.9}] \qquad \ldots (6)$$

where δ_f is film thickness, di is the tube inside diameter, and f is the friction factor for smooth surface.

FILM HEAT TRANSFER WITH PARTIALLY ACTUAL FILM SURFACE

Consider a flat plate of length L whose exposed face is at uniform temperature t and which is inclined at an angle with the horizontal. Fig. 3 illusturates a proposed idealized actual film surface, which can be expressed in the following relation :

$$y_{ax} = y_x \, (1.0 - \xi \sin (2\pi x / p)), \qquad \ldots (7)$$

where x is the distance along the plate in the direction of flow, ξ is a factor less than unity, and p_x is the peiod of the wave. In Eq. (7), y_x is the mean thickness of the condensate film evaluated on the basis of Nusselt theory for laminar film condensation and is given by

$$y_x = \left[\frac{4 k \mu (t_v - t_w)}{\rho (\rho - \rho_v) g h_{fg} \sin \Phi} \right]^{1/4} [x]^{1/4} \qquad \ldots (8)$$

According to Nusselt theory, the local heat transfer coefficient h_x is given by :

$$h_x = k/y_x = \left[\frac{\rho (\rho - \rho_v) k^3 g h_{fg} \sin\Phi}{4 \mu (t_v - t_w)} \right]^{1/4} (1/x)^{1/4} \qquad \ldots (9)$$

To calculate the actual heat transfer coefficient h_{ax} due to the actual surface structure one substitutes in Eq. (9) for y_{ax} instead of y_x^{ax}.

The average actual heat transfer coefficient h_a for the plate of length L is given by :

$$h_a = (1/L) \int_0^L (k/y_{ax}) \, dx = (k/L) \int_0^L \frac{d x}{y_x (1 - \epsilon \sin (2\pi x /p))} \qquad \ldots (10)$$

Since y is function of $x^{1/4}$, the above integration can be performed only numerically. In the present work, numerical integration is performed using the trapezoidal rule. On the other hand, the integration can be performed analytically for $\epsilon = 0$ (smooth surface), the result is given by :

$$h = 0.943 \left[\frac{\rho (\rho - \rho_v) k^3 g h_{fg} \sin\Phi}{L \mu (t_v - t_w)} \right]^{1/4} = 3/4 \, h_L \qquad \ldots (11)$$

To investigate the effect of the proposed actual surface structure described by Eq. (7), condensation over a 1 ft high vertical plate is considered, whose surface is maintained at 71 C. Vapor phase is steam at 0.52 bar and condenses in a filmwise manner. The following property information is used :

$t_v = 82$ C , $t_w = 71$ C , $k = 670 \times 10^{-3}$ W/m degree

$h_{fg} = 2303$ Kj/kg $\mu = 3510 \times 10^{-7}$ kg/m sec.

$\rho = 970.5$ kg/m^3 $g = 9.81$ m/ sec^2 .

In this analysis, liquid properties are assumed to be independent on the temperature.

RESULTS AND DISCUSSION

Analytical solution of the problem obtained according to Nusselt theory for smooth surface ($\epsilon = 0.0$) give the results which are plotted in Fig. 4. The figure illusturates the behaviour of the local heat transfer coefficient h and the local condensate film thickness y along the plate. According to the figure, the minimum heat transfer coefficient occurs when x is maximum, that is when $x = L$. The minimum heat transfer coefficient is 5960 W/m^2 C. The average heat transfer coefficient for smooth film surface given by Eq. (11) is 7948 W/m^2 C.

On the other hand, Fig. 5 illusturates the effect of the actual film surface on the behaviour of the film thickness and heat transfer for certain surface parameters- $\epsilon = 0.2$ and $p = 1/3$ (the wave is repeated 3 times). It is clear that the local film thickness y obyes the function x 1/4 sin (2π x/p), which means local thinning or thickening of the film. Local heat transfer coefficient ($h_{\alpha x}$ = $k/y_{\alpha x}$) has also a wave character.

Most noticeable is the value of the actual average heat transfer coefficient h . The predicted value of h for ϵ = 0.2 and p = 1/3 is 8220 W/m² C, which is 3.2% higher than that obtained for smooth surface (h = 7962 W/m² C) by the same numerical technique. For the same ϵ (0.2) and if p = 1 (one wave over the length of the plate), the predicted value of h is 8282 W/m²C, which is 4% higher than that for smooth surface. This result is physically acceptable because as p increases the film surface becomes more flat (Fig. 6).

When p = 1 and ϵ = 0.5, the predicted value of the actual average heat transfer coefficient h is 9582 W/m²C, which is approximatlly more than 20% higher than that obtained for smooth surface. It is concluded that the parameter is more effective than the parameter p. Predicted values of the actual average coefficients for different surface parameters are listed in the table below. In the extereme case, where ϵ = 0.9, the average heat transfer rates approaches the value of 19465 W/m²C, which is in the order of heat transfer coefficients in case of dropwise condensation.

Table : Average heat transfer coefficients for different actual surface parameters, W/m²C.

$\downarrow \epsilon$ \ p $\rightarrow$	1/3	1/2	1
0.0	7962	7962	7962
0.1	8055	8061	8084
0.2	8220	8242	8282
0.5	9424	9480	9582
0.9	19040	19139	19465

CONCLUSION

In filmwise condensation, actual heat transfer rates are substantially higher than predicted ones. One reason for this descrepancy is the actual surface of the condensate film. Actual films flow in a rippled manner, whose effect on the dry gas heat transfer is compared with the surface roughness. The effect of the actual surface on the film heat transfer is to increases the average coefficients up to 20% higher than coefficients for smooth film surface.

REFERENCES

1- Hestroni, G. : "Handbook of multiphase systems" Hmisphere publishing corporation, 1982

2- Gebhart, B.: "Heat Transfer" McGraw-Hill Book Company, 1971

3- McNaught, J.M.: "An assessment of design methods for condensation of vapors from a noncondensing gas", Heat Exchangers: Theory and Practice, Hemisphere publishing corporation, 1983 .

4- Loser, T.: "Grundlagen für die Berechnung der Teilkondensation von Zwei-und Mehrstoffgemischen in Senkrechten und waagerechten Rohren". Dresden, Technische Universität, Dr. Ing. Diss. 1981

5- Deo, P., V., and Webb, D.R. "An experimental investigation of the effect of waves on vapor side heat and mass transfer in fimwise condensation inside a vertical tube". Int. J. Multiphase flow, Vol. 9, No. 1, pp37-48, 1983

NOMENCLATURE

c_p	specific heat
f	friction factor
g	gravitational acceleration
h	heat transfer coefficient
h_{fg}	latent heat
k	thermal conductivity of liquid phase
L	plate length
q	heat flux
t	temperature
x	distance along the plate
y, δ_f	thickness of the condensate film
ξ, p	film surface parameters
μ	vescosity
ρ	density
ϕ	angle of inclination
Re	Reynolds number
Pr	Prandtle number
Nu	Nusselt number

Subscripts

a	actual
v,g	vapor
w	wall
f	film

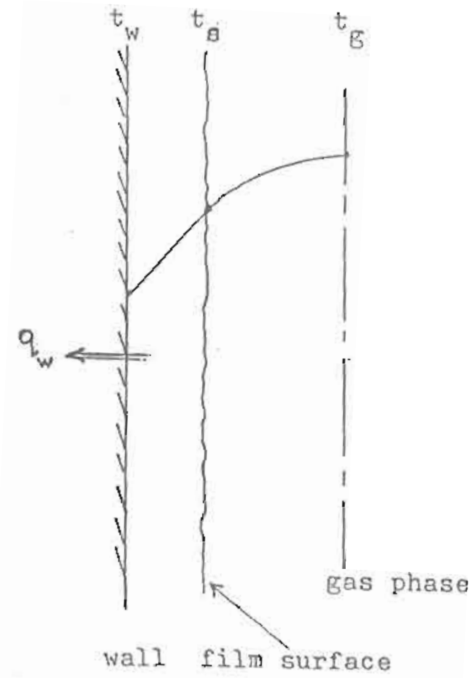

Fig.1 Temperature distribution in partial or total condensers

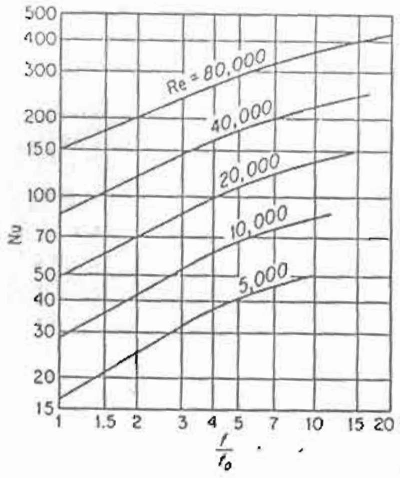

Fig.2 Relation between heat transfer and flow loss[2].

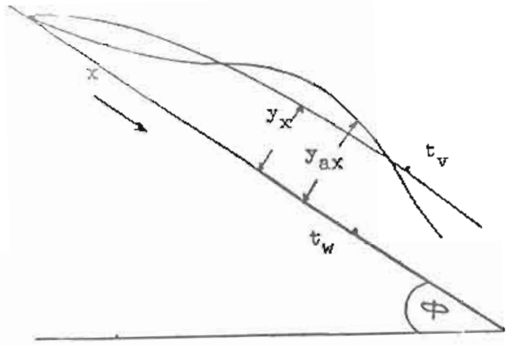

Fig.3 The proposed actual surface nature of the condensate film for laminar condensation on a plate

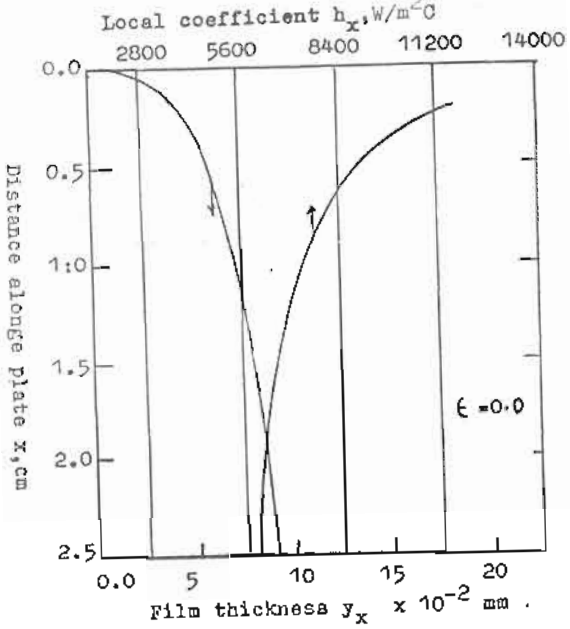

Fig.4 Local surface coefficient and film thickness for laminar film condensation of steam on avertical plate(smooth surface)

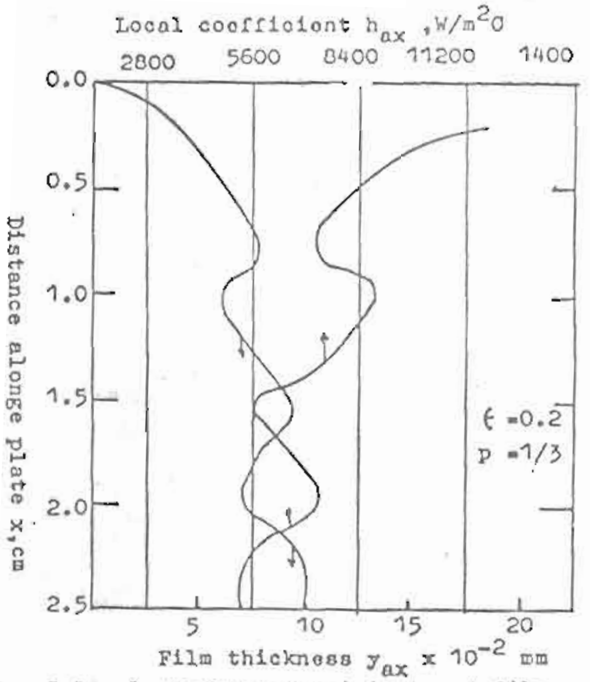

Fg..5 Local surface coefficient and film thickness for laminar film condensation of steam on a vertical plate(rough surface)

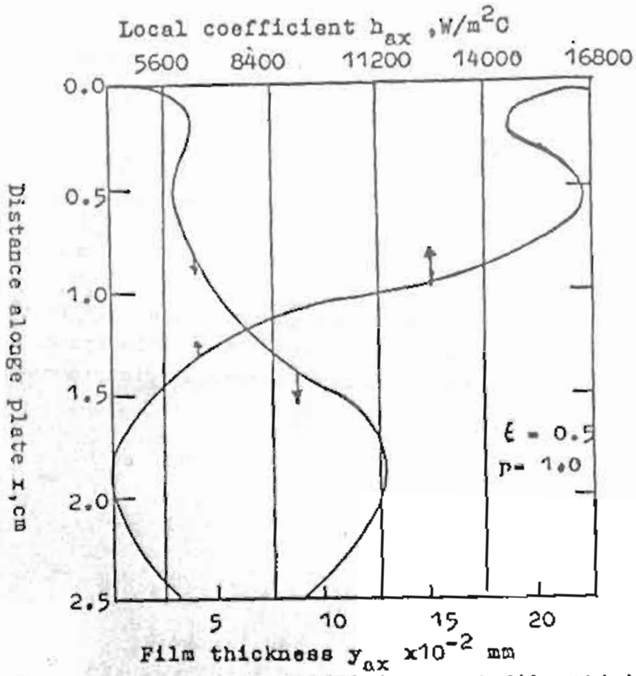

Fig.6 Local surface coefficient and film thickness for laminar condensation of steam on a vertical plate (rough surface)

COMPUTER ROLE FOR DETERMINATION OF FILM COOLING EFFECTIVENESS OF AN AEROFOIL MODEL

BY

Dr. Samir F. Hanna
Faculty of Engineering
EL-MANSOURA UNIVERSITY

Prof. Dr. O.A. AZIM
EL-MINIA UNIVERSITY

Prof. Dr. M.M. AWAD
Head of Mech. Eng. Dept.

N. SH. MATTA

دور الحاسب الآلي في ايجاد معامل التبريد الغشائي لنموذج ايروفويل

خلاصه: يقدم هذا البحث برنامج حاسب آلي لايجاد معامل التبريد الغشائي لنموذج "ايروفويل" وطريقة التبريد المتبعة في هذه الحالة هي بحقن المبرد من خلال صفوف انابيب عند مقدمة حافة نموذج ايروفويل وتتم في وجود وعدم وجود تدرج ضغطي • وقد اجريت الدراسة لحالتي الحقن العمودي والمماسي للسطح وكذلك لظروف زاوية هبوب موجبة وسالبه وزاوية صفر • بواسطة هذا البرنامج يمكن حساب معامل التبريد الغشائي في زمن اقل من عشر ثوان •
والنتائج التي حصل عليها من الحاسب بينت توافقا مرضيا مع النتائج التي حصل عليها من التجارب المعمليه في البحوث السابقة النشر لمعامل التبريد الغشائي للحالات السابقة الذكر •

ABSTRACT - This work presents a FORTRAN computer program for the analysis of film cooling effectivenss of an aerofoil model. The procedure of cooling is by injecting the coolant through a row of tubes at the leading edge of the aerofoil model. The study is carried out for two cases of normal and tangential injection and for zero, positive, and negative attack angle.

The data analysis carried shows satisfactory agreement with experimental results on film cooling effectiveness obtained in previous studies.

NOMENCLATURE

c_f	skin friction coefficient without injection	
c_{pc}	specific heat at constant pressure,	J/(kg.K)
c_p	specific heat at constant pressure for main air stream.	J/(kg.K)
C_p	surface pressure coefficient; $(p-p_\infty)/0.5.\rho.u_\infty^2$	
D	diameter of injection holes,	mm
F.C.F.C.	full coverage film cooling	
h	heat transfer coefficient, $= (k/x)\ S_p.Re_x\ .\ (c_f/2)^{0.5}$	$W/m^2.K$
k	thermal conductivity,	W/m.K
L	chord length of the aerofoil model,	mm
P_s	static pressure,	N/m^2
p	surface pressure,	N/m^2
M	blowing ratio or blowing parameter; $\rho_c.u_c/\rho_\infty.u_\infty$	
m	mass flow rate,	kg/s
Nu	Nusselt number; $(h.x/k) = Re_x\ (c_f/2)^{0.5}.Sp$	
Pr	Prandtl number;	

Re_x	Reynolds number $(u_\infty . x / \nu_\infty)$	
St	Stanton number; $(N_u / Re_x . Pr)$	
t	temperature,	^oC
t_{aw}	adiabatic wall temperature,	^oC
u	local velocity,	m/s
x	distance in streamwise direction,	mm
X	dimensionless distance = x/L	

GREEK LETTERS

η	film cooling effectiveness; $(t_w - t_\infty) / (t_c - t_w)$	
δ	boundary layer thickness,	mm
δ^*	boundary layer displacement thickness; $= \int_0^\infty (1 - \frac{u}{u_\infty})\, dy$,	mm
τ	shear stress,	N/m^2
ρ	density,	kg/m^3
μ	dynamic viscosity,	$N.s/m^2$
ν	kinematic viscosity,	m^2/s

SUBSCRIPTS AND INDICES

c	injectant
t	total
w	wall
∞	main stream

1- INTRODUCTION

Film cooling technique is widely used in many systems to protect solid surfaces exposed to high temperature gas streams. The coolant injected in the boundary layer acts as a heat sink, reducing the gas temperature near the surface. Applications are numerous, particularly in gas turbine systems [1 : 6] where combustion chamber flame tubes, turbine blades, and other hot parts of the engine used air, usually taken from the exit of engine compressor, for film coolant.

In the leading edge region of a turbine blade there is often a very high surface heat transfer. In this region, film cooling has found widespread use in maintaining suitable skin temperatures.

With film cooling, a coolant is injected locally through the wall in such a way that it creates a film along the surface, thereby protecting the wall from exposure to a hot gas stream. The study is carried out for two cases of normal and tangential injection and for zero, positive and negative attack angle [19, 20].

The major part of the present work is to simplify the determination of film cooling effectiveness using a computer program specially designed for this purpose in the light of several analytical studies [7:14].

The program output agreed well with the present experimental results for an aerofoil model.

The experimental study [21] has been conducted in low-speed, open circuit wind tunnel. A detailed description of the wind tunnel, air injection system is given elsewhere [19:21]. Table 1 shows the range of test conditions as given in [21].

Table 1 EXPERIMENTAL RANGE AS GIVEN IN [21]

MAIN STREAM VELOCITY,	u_∞	20 m.s
MAIN STREAM TEMPERATURE ADJACENT TO THE LEADING EDGE,	T_∞	330 K
TEMPERATURE OF INJECTANT AIR,	T_c	300 K
BLOWING RATE,	M	0.2

2- APPROXIMATE ANALYSIS OF FILM COOLING EFFECTIVENESS

Several authors [2, 9, 10] derived expressions for the temperatures distributions in the boundary layer and for the cooling effectiveness of the hot surfaces. In [2, 10:12] experimental data have been correlated with equations similar to the analytical expressions derived in [2]. In [9,10] the influence of specific heat of both the media has been taken into consideration and assuming a fully developed turbulent boundary layer, the following equation has been drived

$$\eta = \frac{1.9\ Pr^{2/3}}{1.0 + 0.329\ B^{0.8}\ \frac{c_{pm}}{c_{pc}}\ .\ \beta} \qquad (1)$$

where

$$\beta = \left(\frac{\mu_c}{\mu_m}\ .\ Re_c\right)^{-0.25} . \frac{X}{[m.b]}$$

β takes into consideration the influence of blowing angle.

Tribus and Klein [12], acting upon a suggestion of Eckert, considered the secondary fluid as a line heat source at the wall. The magnitude of the source depended on the mass flow, temperature, specific heat, etc., of the injectant fluid. They use Duhamel's theorem to predict the film cooling effectiveness to be:

$$\eta = \frac{5.77\ Pr^{2/3}}{(cp_o/cp_c)\ .\ (\mu_o/\mu_c)^{0.2}}\ .\ X^{0.8} \qquad (2)$$

where

$$X = \frac{x}{M.\bar{h}}\ .\ Re_{\bar{h}}^{-0.25} = \frac{x}{M.\bar{h}}\ .\ \left(\frac{u_c.\bar{h}}{\nu_c}\right)^{-0.25}$$

with $\bar{h}$ slot height, and

$$\eta = (T_w - T_\infty) / (T_c - T_\infty)$$

Later prediction by Librizzi [14] and Kutateladze [13] also considered the secondary fluid as a heat source, they assumed the mainstream and coolant fluid in the boundary layer to be completely mixed. In both of these analysis the actual mass of secondary fluid is assumed to be added to the boundary layer which then grows as a normal turbulent layer on a flat plate. They suggested a heat balance to get the mean boundary layer temperature,

$$m_\infty\ c_{p_\infty}\ T_\infty + m_c\ c_{pc}\ T_c = (m_\infty\ c_{p_\infty} + m_c\ c_{pc}).\ T_w \qquad (3)$$

or

$$\eta = \frac{1.0}{1.0 + (m_\infty\ .c_{p_\infty}/m_c\ .c_{pc})} \qquad (4)$$

Since m_c is measured and c_{p_∞} and c_{pc} are known, the problem reduces to a prediction of the mass flow in the boundary layer which comes from the mainstream, m_∞.

In view of Goldstein and Haji-Sheikh [15,16], the mass flowing within the boundary layer is considered to be composed of two different fluids from two different streams. One is the mass injected per unit time which is completely contained within the boundary layer, m_c. The other is the mass which enters the boundary layer from the mainstream per unit time, m_∞. The total mass per unit time in the boundary layer that passes any position is thus

$$m = m_\infty + m_c \qquad (5)$$

Consider $\hat{T}$ as the bulk temperature of the fluid contained within the boundary layer, T_∞ as the temperature of the free stream and T_c is the temperature of the coolant at the point of injection a heat balance [14] yields the relation

$$(\bar{T} - T_\infty)/(T_c - T_\infty) = (m_c \cdot c_{pc})/(m_c \cdot c_{pc} + m_\infty \cdot c_{p\infty}) \qquad (6)$$

Librizzi [14]assumed T to be the wall temperature and m_∞ to be the mass contained in the boundary layer in the absence of mass injection. According to the definition of $\bar{T}$, one can write

$$(\bar{T} - T_\infty) = \frac{\int_0^\infty \rho . c_p . u . (T - T_\infty)\, dy}{\int_0^\infty \rho . c_p . u . dy} \qquad (7)$$

In order to obtain the bulk temperature, both a temperature profile and a velocity profile must be considered. Downstream from the point of injection, one may assume that the velocity profile is governed by the power law

$$\left(\frac{u}{u_\infty}\right) = \left(\frac{y}{\delta}\right)^{\mathring{n}}, \text{ with } \mathring{n} = \frac{1}{n}$$

Assume the temperature profile to be similar, one can write

$$(\bar{T} - T_\infty) = (T_w - T_\infty)\, G\left(\frac{y}{\delta_T}\right) \qquad (8)$$

where

$$\delta_T = \int_0^\infty \frac{T - T_\infty}{T_w - T_\infty}\, dy \qquad (9)$$

Assuming that the product ρc_p does not vary greatly in the y direction, one obtains;

$$\bar{T} - T_\infty = \frac{\int_0^\infty \rho . c_p . u\, (T - T_\infty)\, dy}{\int_0^\delta c_p . \rho . u .\, dy}$$

Divide both sides by $(T_w - T_\infty)$:

$$\frac{\bar{T} - T_\infty}{T_w - T_\infty} = \frac{1}{(T_w - T_\infty)} \cdot \frac{\rho . c_p \int_0^\infty u .\, (T - T_\infty)\, dy}{\rho . c_p \int_0^\delta u . dy}$$

$$= \frac{\int_0^\infty (y/\delta)^{\mathring{n}} . G(y/\delta T)\, dy}{\int_0^\delta \frac{(y)^{\mathring{n}}}{(\delta)^{\mathring{n}}} . dy}$$

$$= \frac{\overbrace{\int_0^\delta (y/\delta)^{\mathring{n}} . G(y/\delta_T)\, dy}^{I_1} + \overbrace{\int_0^\infty (y/\delta)^{\mathring{n}} . G(y/\delta_T)\, dy}^{I_2}}{\left[\frac{1}{\delta^{\mathring{n}}} . \frac{\delta^{\mathring{n}+1}}{\mathring{n}+1}\right]}$$

$$= \frac{1}{\delta}(\mathring{n} + 1).(I_1 + I_2)$$

Making use with δ_T to perform I_1 and I_2 to have the following form :

$$I_1 = \delta_T\,(\delta_T / \delta)^{\mathring{n}} . \int_{(y/\delta_T)=0}^{(\frac{y}{\delta_T})=(\delta/\delta_T)} (y/\delta_T)^{\mathring{n}} . G(y/\delta_T) . d(y/\delta_T)$$

Also,

$$I_2 = \delta_T \int_{(y/\delta_T)=(\frac{\delta}{\delta_T})}^{(y/\delta_T)=\infty} G(\delta/\delta_T). d(y/\delta_T)$$

$$\frac{\bar{T} - T_\infty}{T_w - T_\infty} = (\mathring{n} + 1)\frac{1}{\delta}\left[\left(\frac{\delta_T}{\delta}\right)^{\mathring{n}+1} \int_0^{(\frac{\delta}{\delta_T})} \left(\frac{y}{\delta_T}\right)^{\mathring{n}} . G\left(\frac{y}{\delta_T}\right) . d\left(\frac{y}{\delta_T}\right) + \left[\frac{\delta_T}{\delta}\right] \int_{\delta/\delta_T}^{\infty} G(y/\delta_T) . d(y/\delta_T) \right] \qquad (10)$$

Finally, substitution of $(\bar{T} - T_\infty)$ in equation (6) yields:

$$\frac{T_w - T_\infty}{T_c - T_\infty} = \frac{1/\lambda}{1 + \frac{c_{p\infty} . m_\infty}{c_{pc} . m_c}} \qquad (11)$$

The turbulent boundary layer on a flat plate has a velocity distribution:

$$\left(\frac{u}{u_\infty}\right) = (y/\delta)^{1/n} \qquad (12)$$

As reported by Schlichting [17], the turbulent shear stress is given by:

$$\frac{\tau_w}{\rho . u^2} = 0.0225 \left[\frac{\nu}{u_\infty . \delta} \right]^{0.25} \qquad (13)$$

and the momentum equation:

$$\frac{\tau_w}{\rho . u_\infty^2} = \frac{d}{dx} \int_0^{\delta} \frac{u}{u_\infty} \left(1 - \frac{u}{u_\infty}\right) dy \qquad (14)$$

Substituting equations (12), (13) into equation (14) leads to:

$$\frac{\delta}{x} = \left[\frac{0.0225}{K} \right]^{0.8} (Re_x)^{-0.2} \qquad (15)$$

where

$$K = \frac{1}{(1/\mathring{n}) + 1} - \frac{1}{(2/\mathring{n}) + 1}$$

and

$$m_{\infty} = \int_0^{\delta} \rho . u. dy ; \quad m_c = \rho . u_c . \bar{h}$$

In the light of **Weighardt** [10] analysis, $G(y/\delta_T)$ may be taken as

$$\text{EXP} -C_2 (y/\delta_T)^{2+\mathring{n}}$$

where

$$C_2 = [\Gamma(\frac{n+3}{n+2})]^{\mathring{n}+2}$$

Reffering back to equations (10), (11)

$$\lambda = (\mathring{n}+1) \left[(\delta_T / \delta)^{\mathring{n}+1} \int_0^{\delta/\delta_T} (y/\delta_T)^{\mathring{n}} . G(y/\delta_T).d(y/\delta_T) + (\delta_T/\delta) \int_{\delta/\delta_T}^{\infty} G(y/\delta_T) . d(y/\delta_T) \right] \quad (16)$$

The next item describes a computer program for marching all calculations of film cooling effectiveness.

3- FORTRAN PROGRAM FOR CALCULATING FILM COOLING EFFECTIVENESS

A FORTRAN computer program called 'MTØ' has been developed that calculates the film cooling effectiveness during a short running time (less than ten seconds).

STRUCTURE OF THE PROGRAM

Program 'MTØ' consists of a driver program and three subroutine:

1- SUBROUTINE SIM   2- SUBROUTINE BMW   3- SUBROUTINE FUN

The driver program sets all the boundary conditions and the input data; streamwise distance, mainstream velocity and temperature, injectant fluid velocity and temperature, injection hole geometery, physical properties of the fluids App. A.

The driver program and the subroutines has been diagramed and listed in App.B&C.

PROGRAM DESCRIPTION:

The first part of the driver program (statement 5 : statement 19) sets up the input data.

Statement 20: statement 38, Gama function estimation according to Stirling's expansion [18] which leads to:

$$\Gamma(z) = e^{-z} z^{z-0.5} \sqrt{2\pi} [1 + \frac{1}{12 z} + \frac{1}{288 z^2} - \frac{139}{51840 z^3} - \frac{571}{2488320 z^4} \quad (z^{-5})]$$

Statement 49 : statement 56, estimating of integration 'I_1' .
Statement 57 : statement 66, estimating of integration 'I_2' .
Statement 67 : end of the driver programm, contains the final results of the film colling parameter and the film colling effectiveness.

PROGRAM OUTPUT:

Sample of the results is shown in App.D.

DESCRIPTION OF PARAMETERS

DH	injection hole diameter
CP	specific heat
UMF	mainstream viscosity
UMC	coolant viscosity
RF	mainstream density
RC	coolant density
UF (II)	mainstream velocity
UC	coolant velocity
REX	Reynolds number
DELTA	boundary layer thickness
EETA	film cooling effectiveness
EM (JI)	blowing ratio
X (II)	streamwise distance
AN (I)	(= EN) = $\mathring{n}$ = 1/n
ALAN	film cooling parameter, (λ)
AN (I) = R	n = 1/n
GAMA (I)	Gama function, (λ)
C (I)	G (y/δ)
CTØW = Q	C_2
Y_1 (I,J)	- (ln G(y/δ)) /C_2
Y_2 (I,J)	y/δ_T
Y_3 (I,J)	I_1
Y_4 (I,J)	I_2

4- CONCLUDING REMARKS

Comparison between theoretically obtained results, in the form of film cooling effectiveness, and the experimental results for the aerofoil model are shown in figures 1(a,b,c) and 2.

For zero pressure gradient, tangential injection gives higher values of film cooling effectiveness than normal injection for $x/L < 0.3$ in both experimental and present program results. For x/L higher than 0.3, experimental film cooling effectiveness increases for the normal injection than tangential injection as shown in figure 1,a. These results agree with the visualization photographs which indicate the effective region of the cooling film delayed a distance nearly 3-diameters downstream the injection hole [22].

For negative pressure gradient both normal and tangential injection give lower values for the film cooling effectiveness than the case of zero pressure gradient due to the deceleration of the flow and the separation effects (Fig. 1,b). Comparison between experimental results and present program results for tangential injection indicate similar slope curves but lower values of film cooling effectiveness in the region of x/L 0.45 in the case of present program results.

In the case of positive pressure gradient the film cooling effectiveness increases at the leading edge than for the case of zero pressure gradient for experimental and theoretical results in the case of tangential injection, than gradually decreases downstream x/L =0.3 (Fig. 1,c).

Also, the present program gives more accurate results than uses the flat plate model as shown in figure 2. This is due to taking into consideration the change in mainstream velocity across the chordwise direction.

REFERENCES

[1] A. Hare, H.H. Malley SAE Trans. Vol. 75, pp. 230-246, 1976

[2] E.R.G. Eckert Analysis of heat and mass transfer, Mc Graw-Hill New York 1972.

[3] R.J. Goldstein, V.L. Eriksen Journal of heat transfer (ASME), pp. 239-245, May, 1974.

[4] M. Hirata J1 Of JSME? Vol. 70, No. 581, pp. 107-113, June, 1974.

[5] A. Iguchi, Proceeding of 17th National Heat Transfer Symposium of Japan, Kanazawa, 1980.

[6] Mitsubishi Tech. Rev. Vol. 19, No. 2, (1982-3)

[7] R.J. Goldstein, J1. of heat transfer, (ASME), Vol. 104, pp. 355-361, May 1982.

[8] R.J. Goldstein, J1. of heat transfer (ASME)? Vol. 104, pp. 715-721, Nov., 1982.

[9] J.L. Stollery, A.A. EL-Ehwany Int. J1. of Heat Mass Transfer, Vol. 8 pp. 55-65, 1985.

[10] K.Wieghardt, 'Hot air discharge for De-Icing', AAF Trans. No. F-TS'919,-RE, 1964.

[11] E.R.G. Eckert, Proceeding of the national heat transfer symposium of Japan, Kanazawa, 1980.

[12] M. Tribus, J. Klein, 'Forced Convection From Nonisothermal Surfaces' Heat Transfer Symposium, University of Michigan press, Ann Arbor, Michigyn 1953.

[13] S.S. Kutateladze, The Heat Transfer In Turbulent Boundary Layer Of A Gas, Thermophysics Inst., Siberian Div. Academy of Sc., USSR, Vol.1 No. 2, pp. 281-290, Sept.-Oct. 1963 (Trans. from Russian)

[14] J. Librizzi, AJAA Jl., Vol. 4, April 1964, pp. 617-623.

[15] R.J. Goldstein, A. Haji-Sheikh, JSME 1967 Semi-International Symposium 4th.-8th. Sept. 1967, Tokyo.

[16] A. Haji-Sheikh, Jl. of heat transfer, (ASME), 1981.

[17] H. Schlichting, Boundary Layer Theory, sixth edition, Mc Graw-Hill, New York.1968.

[18] R.S. Murray Finite differences and difference equations. Mc Graw-Hill Book company, 1971.

[19] S.F. HANNA, M.M. AWAD, O.A. AZIM, N.S.MATTA Injection in boundary layer and its influence on surface pressure coefficients for an aerofoil model. Mansoura University Bulletin, June, 1982.

[20] S.F. HANNA, M.M. AWAD, O.A. AZIM, N.S. MATTA A study of transpiration from perforated flat plate. Mansoura University Bulletin, Vol. 9, No. 1, June, 1984.

[21] Nabil, SH.M. " Full coverage film cooling surface with holes injection in boundary layer and its influence on heat transfer". Ph. Dr. Thesis, Mansoura University 1984.

[22] O.A. AZIM, et. al. Flow Visualization and Thermal Mapping on Film Cooled Turbine Blade Leading Edge. Bulletin of the faculty of engineering & technology, MINIA UNIVERSITY, Vol.3,Part 1, 1984.

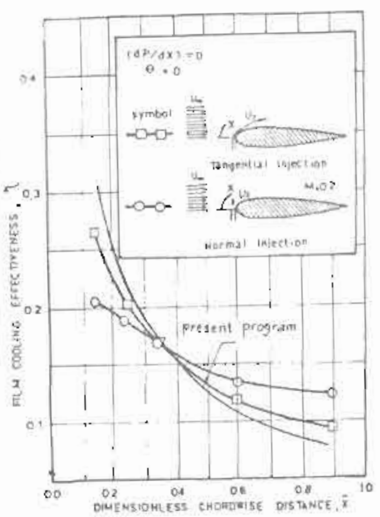

FIG. 1-a, CHORDWISE DISTRIBUTION OF FILM COOLING EFFECTIVENESS

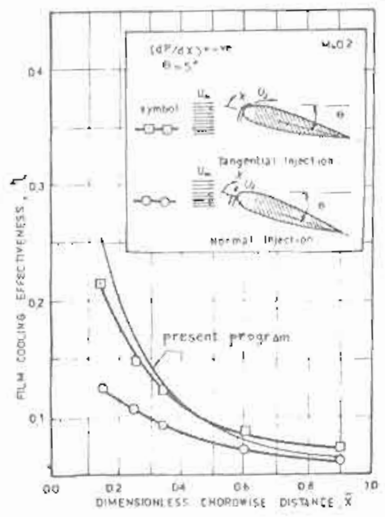

FIG. 1-b, CHORDWISE DISTRIBUTION OF FILM COOLING EFFECTIVENESS

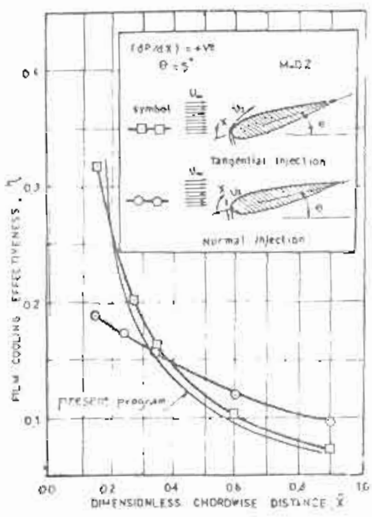

FIG. 1-c, CHORDWISE DISTRIBUTION OF FILM COOLING EFFECTIVENESS

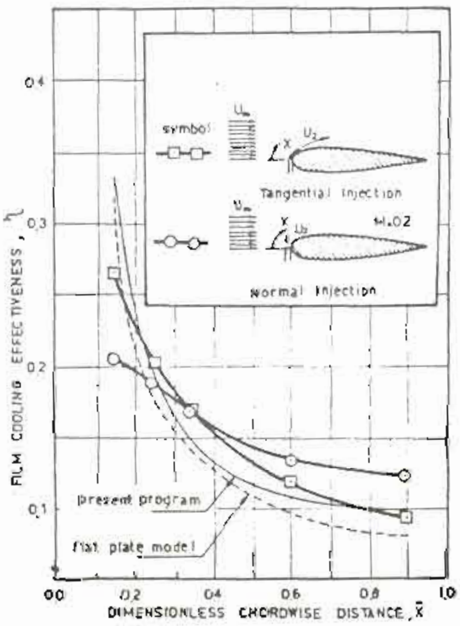

FIG. 2. CHORDWISE DISTRIBUTION OF FILM COOLING EFFECTIVENESS

Appendix A

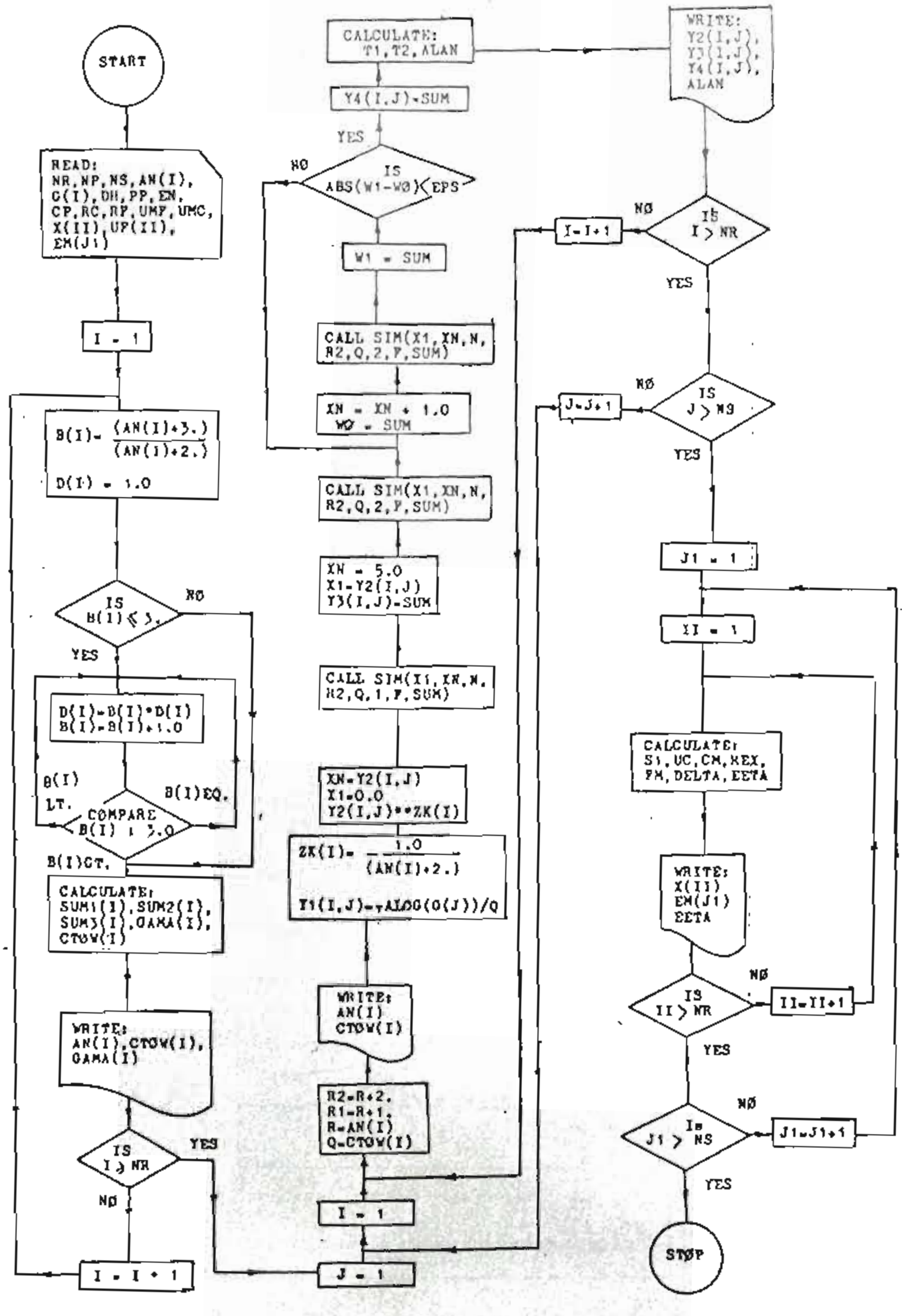

FLOW-CHART FOR FILM COOLING PREDICTION PROGRAM - 'NTO'

Appendix B

```
      SUBROUTINE SIM(X1,XN,N,R2,Q,M,F,SUM)
      DIMENSION F(400)
      N1=N+1
      H=(XN-X1)/N
      DO 3 K=1,N1
      I1=K-1
      X=X1+I1*H
      IF(M.EQ.1)GO TO 10
      CALL BMW(K,R2,Q,X,F)
      GO TO 3
   10 CALL FUN(K,R2,Q,X,F)
    3 CONTINUE
      SUMO=0.0
      SUME=0.0
      DO 4 K=2,N,2
    4 SUMO=SUMO+F(K)
      N6=N-1
      DO 5 K=3,N6,2
    5 SUME=SUME+F(K)
       SUM=H*(F(1)+F(N1)+4.*
     *SUMO+2.*SUME)/3.
       RETURN
       END
```

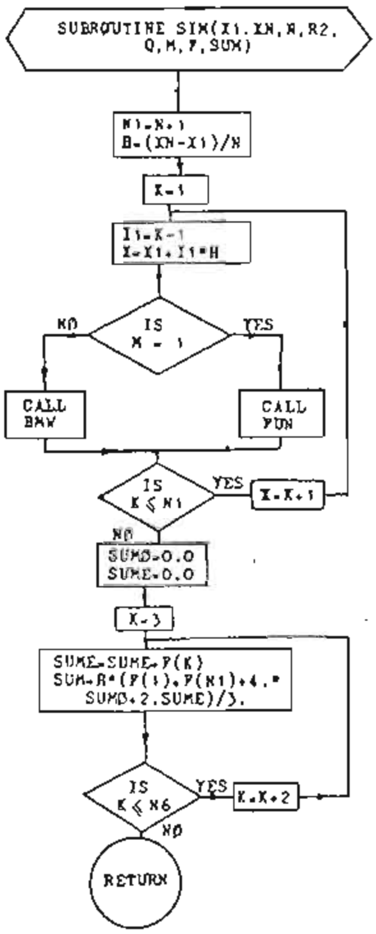

FLOWCHART FOR SUBROUTINE 'SIM(X1, XN,N,R2,Q,M,F,SUM)'.

```
      SUBROUTINE BMW(K,R2,Q,X,F)
      DIMENSION F(400)
      F(K)=0.0
      F(K)=EXP(-Q*(X**R2))
      RETURN
      END
```

```
      SUBROUTINE FUN(K,R2,Q,X,F)
      DIMENSION F(400)
      F(K)=0.0
      SS=EXP(-Q*(X**R2))
      F(K)=(X**(R2-2))*SS
      RETURN
      END
```

Appendix C

```
C       FILM COOLING PREDICTION PROGRAM - 'MTO'
        DIMENSION AN(10),B(10),SUM1(10),SUM2(10),SUM3(10),
       *D(10),GAMA(10),CTOW(10),G(10),C(10),Y1(10,10),
       *ZX(10),Y2(10,10),Y3(10,10),F(400),Y4(10,10),UP(10),
       *EM(10),X(20)
        N = 200
        EPS = 0.000001
        PI = 3.141592653
        PA = SQRT(2.*PI)
        WRITE(2,200)
        WRITE(2,201)
        WRITE(2,200)
        READ(1,4)NR,NP,NS
        READ(1,8)(AN(I),I=1,NR)
        READ(1,9)(G(I),I=1,NR)
        READ(1,5)DH,PP,EN,CP,RC
        READ(1,6)RP,UMP,UMC
        READ(1,7)(X(II),II=1,NS)
        READ(1,7)(UP(II),II=1,NS)
        READ(1,30)(EM(J1),J1=1,NP)
        DO 10 I=1,NR
        B(I)=(AN(I)+3.)/(AN(I)+2.)
        D(I)=1.0
        IF(B(I).GT.3.)GO TO 11
   12   D(I)=B(I)*D(I)
        B(I)=B(I)+1.0
        IF(B(I)-3.)12,12,11
   11   SUM1(I)=1.+1./(12.*B(I)+1./(288.*B(I)*
       *B(I))-139./(51840.*(B(I)**3.))-571./
       *(2488320.*(B(I)**4.))
        SUM2(I)=1./EXP(B(I))
        C(I)=B(I)-0.5
        SUM3(I)=B(I)**C(I)
        GAMA(I)=(SUM2(I)*SUM3(I)*PI*
       *SUM1(I))/D(I)
        ANN=AN(I)+2.
        CTOW(I)=GAMA(I)**ANN
        WRITE(2,202)AN(I),CTOW(I),GAMA(I)
   10   CONTINUE
        WRITE(2,200)
        DO 15 I=1,NR
        Q=CTOW(I)
        R=AN(I)
        R1=R+1.0
        R2=R+2.0
        WRITE(2,203)AN(I),CTOW(I)
        WRITE(2,200)
        WRITE(2,204)
        WRITE(2,200)
        DO 16 J=1,NR
        Y1(I,J)=-ALOG(G(J))/Q
        ZX(I)=1./(AN(I)+2.)
        Y2(I,J)**ZX(I)
        X1=0.0
        XN=Y2(I,J)
        CALL SIM(X1,XN,N,R2,Q,1,F,SUM)
        Y3(I,J)=SUM
        X1=Y2(I,J)
        XN=5.0
        CALL SIM(X1,XN,N,R2,Q,2,F,SUM)
  101   W0=SUM
        XN=XN+1.0
        CALL SIM(X1,XN,N,R2,Q,2,F,SUM)
        W1=SUM
        IF(ABS(W1-W0).LE.EPS)GO TO 100
        GO TO 101
  100   Y4(I,J)=SUM
        T1=R1*((1./Y2(I,J))**R1)*Y3(I,J)
        T2=R1*(1./Y2(I,J))*Y4(I,J)
        ALAN=T1+T2
        WRITE(2,205)Y2(I,J),Y3(I,J),Y4(I,J),ALAN
   16   CONTINUE
        WRITE(2,200)
   15   CONTINUE
        DO 106 J1=1,NS
        DO 105 II=1,NR
        S1=0.2242*DH
        UC=EM(J1)*(RP*UP(II))/RC
        CM=RC*S1*UC
        REX=RP*UP(II)*X(II)/UMP
        DELTA=X(II)*0.37/REX**0.2
        FM=RP*UP(II)*DELTA/(EN+1.)
        EETA=CM*CP/(0.56*FM)
        WRITE(2,36)X(II),EM(J1),EETA
  105   CONTINUE
  106   CONTINUE
    4   FORMAT(3(I2))
    5   FORMAT(5(F7.4,1X))
    6   FORMAT(F4.2,2X,2(F9.7,2X))
    7   FORMAT(5(F6.3,2X))
    8   FORMAT(6(F4.2,2X))
    9   FORMAT(6(F5.3,2X))
   36   FORMAT(3(F8.4,2X))
   30   FORMAT(5(F5.3,2X))
  200   FORMAT(80(1H=))
  201   FORMAT(2X,'N',7X,'C2',8X,'GAMA')
  202   FORMAT(F5.3,2(1X,F10.5))
  203   FORMAT(2X,'N',F5.3,2X,'C2=',F10.5)
  204   FORMAT(1X,'Y/DELTA',2X,'INTEGRAL 1',2X,
       *'INTEGRAL 2',5X,'LANDA')
  205   FORMAT(4(F10.5,2X))
        STOP
        END
```

Appendix D

SAMPLE OF THE OUT PUT RESULTS OF'MTØ'.

M	C2	GAMA
0.120	0.77302	0.88565
0.140	0.77109	0.88562
0.150	0.77014	0.88561
0.160	0.76919	0.88560
0.180	0.76733	0.88561
0.200	0.76550	0.88562

M=0.120 C2=0.77302

Y/DELTA	INTEGRAL 1	INTEGRAL 2	LANDA
2.32055	0.90373	0.00217	0.39532
2.08998	0.89973	0.00597	0.44454
1.89455	0.89219	0.01307	0.49623
1.76894	0.88394	0.02083	0.53583
1.67339	0.87514	0.02915	0.57015
1.59483	0.86586	0.03796	0.60160

M=0.140 C2=0.77109

Y/DELTA	INTEGRAL 1	INTEGRAL 2	LANDA
2.30506	0.89050	0.00213	0.39286
2.07806	0.88648	0.00588	0.44220
1.88547	0.87892	0.01287	0.49405
1.76160	0.87068	0.02053	0.53380
1.66730	0.86190	0.02873	0.56826
1.58975	0.85264	0.03743	0.59905

M=0.160 C2=0.76919

Y/DELTA	INTEGRAL 1	INTEGRAL 2	LANDA
2.28992	0.87769	0.00209	0.39047
2.06639	0.87365	0.00579	0.43991
1.87657	0.86609	0.01268	0.49192
1.75438	0.85786	0.02023	0.53181
1.66132	0.84910	0.02833	0.56641
1.58474	0.83986	0.03692	0.59813

M=0.180 C2=0.76733

Y/DELTA	INTEGRAL 1	INTEGRAL 2	LANDA
2.27510	0.86529	0.00206	0.38813
2.05496	0.86124	0.00570	0.43768
1.86784	0.85368	0.01249	0.48984
1.74730	0.84546	0.01994	0.52986
1.65544	0.83671	0.02794	0.56459
1.57982	0.82751	0.03642	0.59644